https://doi.org/10.17221/125/2022-JFS

Assessment of aboveground biomass and carbon stock of subtropical pine forest of Pakistan

Nizar Ali[1], Muhammad Saad[1], Anwar Ali[2], Naveed Ahmad[3], Ishfaq Ahmad Khan[4], Habib Ullah[5], Areeba Binte Imran[3]*

[1]Department of Forestry and Wildlife Management, University of Haripur, Haripur, Pakistan
[2]Pakistan Forest Institute Peshawar, Peshawar, Pakistan
[3]Department of Forestry and Range Management, University of Arid Agriculture Rawalpindi, Rawalpindi, Pakistan
[4]Department of Forest Science & Biodiversity, Faculty of Forestry and Environment, University Putra Malaysia (UPM), Serdang, Malaysia
[5]School of Forestry, North-East Forestry University, Herbin, China

**Corresponding author: ishfaqahmad860@gmail.com*

Citation: Ali N., Saad M., Ali A., Ahmad N., Khan I.A., Ullah H., Imran A.B. (2023): Assessment of aboveground biomass and carbon stock of subtropical pine forest of Pakistan. J. For. Sci., 69: 287–304.

Abstract: The presented study estimated the aboveground biomass (*AGB*) of *Pinus roxburghii* (chir pine) natural forests and plantations, and created biomass maps using a relationship (regression model) between *AGB* and Sentinel-2 spectral indices. The mean *AGB* and *BGB* (belowground biomass) of natural forests were 79.54 Mg·ha^{-1} and 20.68 Mg·ha^{-1}, respectively, whereas the mean *AGB* and *BGB* of plantations were 94.48 Mg·ha^{-1} and 24.56 Mg·ha^{-1}, respectively. Correlation showed that mean diameter at breast height (*DBH*) and mean height have weak relationships with *AGB*, and *BGB* has shown correlation coefficients (R^2 = 0.46) and (R^2 = 0.56) for polynomial models. Regression models between *AGB* (Mg·ha^{-1}) of *Pinus roxburghii* natural forest and Sentinel-2 spectral indices showed a strong relationship with Ratio Vegetation Index (*RVI*) with R^2 = 0.72 followed by Normalized Difference Vegetation Index (*NDVI*) and Atmospherically Resistant Vegetation Index (*ARVI*) with R^2 = 0.70. In contrast, the lower performance of spectral indices has been shown in regression with plantation *AGB*. Correlation coefficients (R^2) were 0.41, 0.41, and 0.40 for *RVI*, *NDVI*, and *ARVI*, respectively. All indices showed that the distribution of *AGB* data was not the best fit with the linear regression model. Therefore, non-linear exponential and power models were considered the best fit for *NDVI*, *RVI*, and *ARVI*. A biomass map was developed from *RVI* for both natural forests and plantation because RVI has the highest R^2 and lowest *P*-value.

Keywords: natural forest; *Pinus roxburghii*; plantations; regression analysis; Sentinel-2; vegetation index

The world forest has spread around 4.06 billion ha, which accounts for 31% of the total area and has been showing a decreasing trend for the last three decades (FAO 2020). The world's forest land is believed to have declined from 31.6% to 31.0% of the total area (Jallat et al. 2021). Human intervention on a large scale is the main factor in reducing the world's forests (FAO 2020; Kyere-Boateng, Marek 2021). Deforestation and forest degradation contribute to global climate change (GCC) by releasing carbon into the atmosphere, which has detrimental effects on the environment. In this context, world forests are crucial since they function as a carbon sinker and carbon source (Raihan et al. 2019; Huang et al. 2020; Babbar et al. 2021).

https://doi.org/10.17221/125/2022-JFS

The forest's role in removing carbon from the atmosphere and GCC mitigation has been fully acknowledged (Houghton et al. 2015). Reducing or reversing forest degradation in (sub)tropical regions will contribute to GCC mitigation, given the significant impacts of forest degradation on global biodiversity and ecosystem services, including carbon sequestration (Nyamari et al. 2021; Thammanu et al. 2021). The extent of forest biomass determines ecosystem productivity. It is used to evaluate the function of vegetation in the carbon cycle, its energy production capacity, and the carbon stock assessment for climate change modelling (Siddiq et al. 2021). Due to the high potential of carbon dioxide (CO_2) storage, the forest's role as a carbon sink has long been recognised as the most significant one, as forests hold most of the above- and belowground terrestrial regenerative carbon (Zhang et al. 2013). Nevertheless, at the global level, the soil is considered the largest carbon pool compared to other major terrestrial ecosystems such as forests (Zhang et al. 2021). Aboveground biomass (*AGB*) comprises stems, stumps, branches, bark, seeds, and leaves; belowground biomass (*BGB*) contains all active roots with a diameter greater than 2 mm; and the dead mass of coarse and fine aggregate attached to the soil. The more easily measured *AGB* can be used to estimate the other terrestrial carbon pools. As a result, *AGB* has typically been the focus of biomass estimation research (Goetz, Dubayah 2011). Hereafter, the term 'forest biomass' is used to indicate forest *AGB*.

Forest biomass can be estimated through destructive or non-destructive methods (Khan et al. 2021a). The destructive method is generally not favoured as it is costly, laborious, limited in spatial and temporal samplings, and may have a negative effect on forest health (Qureshi et al. 2012). The non-destructive method comprises physiological-based models, carbon flux measurements, forest yield models, forest inventory-based approaches, and remote-sensing methods (Qureshi et al. 2012). Furthermore, remote sensing products such as Sentinel-2 can provide spatially clearly defined and precisely combined information about forest biomass quantity at the broad level of spatial and temporal resolutions by frequent revisit time of 10 days for a single Sentinel-2 satellite and 5 days for constellation and usage of historical data archives (Nhangumbe et al. 2023). The assessment of forest biomass can be greatly improved by using satellite data such as Sentinel-2 images, which offer superior spectral coverage, spatial resolution, and temporal frequency compared to other platforms (Shoko, Mutanga 2017). The Sentinel-2 platform boasts a multispectral instrument (MSI) sensor that captures images with a wider range of spectral coverage, including red-edge and shortwave infrared bands, as well as higher spatial resolution (10 m, 20 m, 60 m) and more frequent temporal coverage than Landsat (Sun et al. 2019; Isbaex, Coelho 2021; Ahmad et al. 2023). Sentinel-2 imagery is open-source data that can be acquired freely from the European Space Agency (ESA) hub. Its use has improved the integration of biomass modelling with vegetation indices, spectral bands, and biophysical variables based on field-measured data (Castillo et al. 2017; Zhang et al. 2017). The red-edge band present in Sentinel-2 product is particularly well-suited for mapping and assessing vegetation characteristics (Shoko, Mutanga 2017; Pertille et al. 2019; Ahmad et al. 2023). Among remote sensing technologies, Synthetic Aperture Radar (SAR) has proven to be the most sensitive in retrieving forest biophysical parameters such as canopy height and aboveground biomass (Khati et al. 2017; Musthafa et al. 2020), with SAR backscatter being the most commonly used parameter for biomass retrieval. In recent years, Light Detection and Ranging (LiDAR) has gained significant traction as a complementary remote sensing tool for forest biophysical parameter retrieval, as it provides highly accurate three-dimensional forest structures (Musthafa, Singh 2022).

Although remote sensing is unlikely to provide more precise biomass estimates at the plot or stand level in the mid-term, it is equally unlikely that field-based inventories can effectively address the systematic, wall-to-wall mapping at regional or larger scales. Nonetheless, field-based biomass assessments are crucial for remote-sensing methodologies for calibrating models and validating results (Ahmad et al. 2023).

Pakistan has a low forest cover of about 5% of the total land area, with most of the forest in the country's northern region (Bukhari et al. 2012; Khan et al. 2021a). Various evergreen trees of the *Pinaceae* family, including the *Pinus roxburghii*, are present in the Himalayas and can be found in Pakistan, India, Nepal, and Bhutan. There are approximately 105 *Pinus* species present in the world (Satyal et al. 2013); out of these, six species occur in Pakistan: *Abies pindrow, Cedrus deodara, Picea smithi-*

https://doi.org/10.17221/125/2022-JFS

ana, Pinus gerardiana, Pinus roxburghii, and *Pinus wallichiana. Pinus roxburghii* is a coniferous tree that may grow to a height of up to 55 m with a stem diameter reaching up to 2 m (Satyal et al. 2013). *Pinus roxburghii* has a long rotational age and a high carbon sequestration potential. In Kashmir Himalaya, Pakistan, the *AGB* of a mature Chirpine forest was estimated to be 191.8 Mg·ha^{-1} (Shaheen et al. 2016). Another study in Azad Jammu and Kashmir (AJK) reported the average carbon stock potential of chir pine to be 5.93 Mg·ha^{-1} (Khan et al. 2021b). *Pinus roxburghii* is the most dominant *Pinus* species in Buner district. The main objectives of this study were (*i*) to evaluate aboveground dry biomass (*AGB*) of *Pinus roxburghii* natural forests and plantations in the study area, and (*ii*) to develop a relationship (regression model) between aboveground biomass and Sentinel-2 spectral indices to generate biomass maps.

MATERIAL AND METHODS

The study area – Buner Forest Division. Buner Forest Division is the study area of the current research. It is located at the coordinates of 34°10'N and 34°43'N, and 72°11'E and 72°49'E (Figure 1). Different types of forests can be found in the area, including dry subtropical broadleaved, pure chir pine, dry oak (*Quercus baloot*), and mixed chir and kail forests. The forest inventory for the present study was conducted mainly in chirpine forests that fall in submature category i.e. 40 years. These forests extend from 1 000 m a.s.l. to 1 500 m a.s.l. and occupy a vast majority of the Gadazai, Malik Pur, Batai, Karakar, Daggar, Chamla, Nagri, Mohaban, and Malka areas. The broadleaved species that exist in these forests are Kao (*Olea cuspidata*), *Ficus* spp., batangi, white oak, sanatha (*Dodonaea viscose*), *Celtis australis*, *Rubus* spp., gurgura (*Monotheca buxifolia*), and bhekar (*Adhatoda vassica*) etc. The mean annual temperature, mean annual precipitation and relative humidity of the study area are recorded as 19 °C, 1 068 mm, and 60–65% respectively (Rahman et al. 2022). The plot-wise coordinates, elevation (m), slope (degrees), and aspect (degrees) are summarised in Table S1 in the Electronic Supplementary Material (ESM). Regarding natural forests, the elevation ranges from 795 to 1 885 m, while the slope ranges from 10.45 to 48.57 degrees. Similarly, aspects range from 1.64 to 359.37 degrees. Likewise, mean elevation, aspect, and slope were 1 180.10 ± 63.27 m a.s.l., 28.15 ± 23.43 degrees, and 173.53 ± 2.03 degrees, respectively. On the other hand, in the case of plantations, the highest elevation, slope, and aspect for natural forests were 1 707 m a.s.l., 42.51 degrees, and 349.05 degrees, respectively. The lowest elevation, slope and aspect were 699 m, 4.39 degrees, and 15.85 degrees, respectively. At the same time, the mean elevation, slope, and aspect were 923.32 m ± 53.20, 23.29 ± 2.25 degrees, and 243.39 ± 21.4 degrees, respectively.

Forest inventory. Table 1 below shows various instruments used for field sampling for *AGB*, including satellite images.

Field data were collected from 57 sample plots during January 2020 for biomass and carbon stock estimation. The random sampling design was adopted during inventory. 29 plots were from the natural forest of *Pinus roxburghii*, and 28 plots were from the plantation of *Pinus roxburghii*, re-

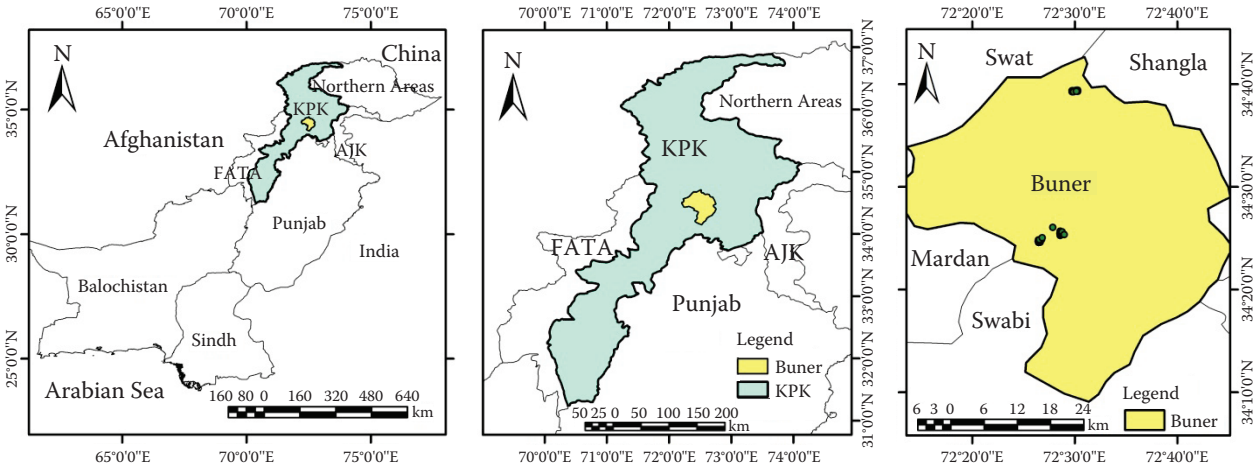

Figure 1. Study area map

https://doi.org/10.17221/125/2022-JFS

Table 1. Tools used in field sampling

Materials	Purpose	Unit
Diameter caliper (120 cm)	diameter measurement	cm
Haga altimeter	height measurement	m
Sunnto clinometer	slope and height measurement	degrees and m
Measuring tape (100 m)	measuring distance	m
Ranging rods	plot centre and other location	–
Garmin GPS	navigation	degree, minute, second
Sentinel-2 image	computation of vegetation indices and biomass	ratio

spectively. Each plot was circular with a radius of 17.84 m and an area of 0.1 ha, all of them being distributed in the Buner Forest Division. Tree height and diameter at breast height (*DBH*) were measured in all plots to calculate aboveground biomass (Afzal, Akhter 2011; Nizami 2012). All trees with a *DBH* of ≥ 5 cm were measured. Diameter calliper of 120 cm length was used to measure *DBH*. As per UNFCCC guidelines (Nizami 2012; Ahmad et al. 2023) regarding tree measurement, forked and defective trees were also subjected to measurement as they are believed to have a quantity of biomass (Ali et al. 2018). Haga Altimeter used for height measurement is a gravity-oriented pointer device for height measurement within a fixed range of distances (20 m, 25 m, and 30 m). As height measurement is difficult and time-consuming for variable distances and viewpoints, it was only measured for dominant trees in the plots. Suunto Clinometer (Finland) was used for slope estimation, the distance was measured with the help of a measuring tape (100 m), and GPS (Garmin, USA) was used for location identification or navigation purposes. Compass was used for the proper direction of plot selection in the area for aspect identification. During the field survey, selected samples included maximum variability of available *DBH* and height groups in homogeneous forest regions for each species.

For tree height estimation, the following Equation (1) was used:

$$H = \tan\theta \times b + a \quad (1)$$

where:

H – total height of a tree (m);
θ – angle of a tree to the top of the tree from observers' eyes;
b – distance between the tree base and the observer (m);
a – observer eye height (m).

Full enumeration and direct measurement of *AGB* through destructive sampling is considered the most accurate; however, such methods are costly and laborious (Kumar, Mutanga 2017). Regression models (allometric equations) provide effective alternatives to destructive sampling (Seidel et al. 2011). These equations convert inventory data into an estimate of aboveground biomass. A literature survey was conducted for the selection of species-specific as well as general allometric models. Biomass carbon contents of each species differ from others due to specific wood density and properties (Lamlom, Savidge 2003).

Biomass estimation. Pool 1: Aboveground biomass (*AGB*).

Method 1: Using *BEF* (biomass expansion factor) (Ali et al. 2020b) [Equation (2)]:

$$AGB = V \times WD \times BEF \quad (2)$$

where:

AGB – aboveground biomass;
V – volume;
WD – wood density [available from literature (Ali et al. 2018)];
BEF – biomass expansion factor [available from literature (Ali et al. 2018)].

Method 2: Using allometric equation.

Aboveground biomass (*AGB*) was estimated by allometric equation in two steps (Ali et al. 2020a) [Equations (3–4)]:

$$H = 0.0044 \times DBH^2 + 0.686\ DBH - 0.7196 \quad (3)$$

$$AGB = 0.0224\ (DBH^2 \times H)^{0.9767} \quad (4)$$

where:

AGB – aboveground biomass (kg);
DBH – diameter at breast height (cm);
H – height (m).

https://doi.org/10.17221/125/2022-JFS

Pool 2: Belowground biomass (*BGB*) (Ali et al. 2020b) [Equation (5)]:

$$BGB = AGB \times R/S \quad (5)$$

where:

BGB – belowground biomass;

R/*S* – root-shoot ratio [available from literature (Ali et al. 2017)].

The species-wise aboveground and belowground biomass were estimated by summing up the tree biomass values (kg) calculated for each plot. According to a plot size of 1 000 m^2, the plot-based *AGB* (Mg) were converted to standard *AGB* units per hectare by multiplying by a scaling factor of 10. The plot-based *AGB* and *BGB* values were given in kg, then converted to Mg by dividing by 1 000.

The Intergovernmental Panel on Climate Change (IPCC) explains how to calculate changes in carbon stocks, greenhouse gas emissions, and biomass content in forest areas using various methodologies. Typically, carbon accounts for around half of the dry biomass (Malhi et al. 2004). Thus, the carbon stock can be estimated by multiplying the dry biomass by 0.47 (Ali et al. 2020b). Belowground biomass was calculated by multiplying the *AGB* by 0.26 according to IPCC guidelines (Ravindranath, Ostwald 2008). Aboveground carbon stocks (*AGC*) and belowground carbon stocks (*BGC*) were calculated by multiplying the dry biomass (aboveground and belowground) by 0.47 (Afzal, Akhter 2011). After that, the carbon stock was multiplied by 44/12 (the carbon atom ratio in the molecular weight of CO_2) to get the CO_2 equivalent value (Pearson et al. 2007).

Remote sensing. The current study used a Sentinel-2 image for *AGB* estimation; the Sentinel-2 image was acquired from Copernicus Sentinel Scientific Data Hub (https://scihub.copernicus.eu/) on Jan 13, 2020. Pre-processing of Sentinel-2 image was the first step before using it for biomass estimation purposes. The aim was to avoid the effects of atmospheric scattering or cloud cover shadows, visual aid interpretation, and extract plenty of information from remotely sensed images. Preprocessing included radiometric, geometric, and terrain corrections. Sentinel Application Platform (SNAP 5.0, 2016) is a toolbox used for analysis and processing of Sentinel-2 images. Sen2Cor is a third-party plugin in SNAP 5.0, used for preprocessing of Sentinel-2 Level-1C raw image into Level-2A rectified image. Atmospheric correction comprised of bottom-of-the atmosphere (BoA) reflectance and top-of-the-atmosphere (ToA) reflectance. Sentinel-2 Level-1C was processed by Sen2Cor plugin, starting with cloud correction and classification, followed by aerosol particle thickness and retrieval of water vapours; ultimately the process ended with Level-2A output. The subsetting of rectified images has been done up to the extent of the research area where forest inventory was carried out. In order to calculate the average value for the plot, mean filter of 3 × 3 matrixes has been run on Sentinel-2 image to resample it as per field sample plot size. Further, different vegetation indices were computed using SNAP for Sentinel-2 images, respectively (Table 2). These indices indicate biomass potential and the health of the vegetation. *AGB* shapefile created via ArcGIS 10.3 (2014) was overlaid on corresponding vegetation indices of both the acquired images. The values of masked pixels (where field data was overlaid) were extracted for all the indices, and mean values were calculated.

Statistical analysis. Different explanatory variables explain total carbon sequestered and carbon in other pools (above- and belowground). These variables and their analysis include *DBH* versus height, *AGB* versus *DBH*, and *AGB* versus height. Moreover, scatter plots were also created to examine the association between biomass and individ-

Table 2. Sentinel-2 vegetation indices

Indices	Sentinel-2 bands	Reference
Normalized Difference Vegetation Index (*NDVI*)	(Band 8 – Band 4) / (Band 8 + Band 4)	Rouse et al. (1973)
Atmospherically Resistant Vegetation Index (*ARVI*)	((Band 8–Band 4 – (Band 2 – Band 4)) / (Band 8 + + Band4 – (Band 2 – Band 4))	Kaufman, Tanre (1992)
Ratio Vegetation Index (*RVI*)	(Band 8) / (Band 4)	Tucker (1979)

https://doi.org/10.17221/125/2022-JFS

ual indices. The coefficient of determination (R^2), *RMSE* (root mean square error), and *P*-value were calculated for each model in SPSS 16.0 (2007). As a result, the model fulfilling the conditions of high R^2, low *RMSE*, and ($P < 0.05$) was selected for effective biomass estimation and generation of biomass map in ArcGIS (Version 10.3, 2014).

RESULTS

Tree attributes of natural forests. Mean *DBH* and mean height was determined for each natural forest plot, and the mean values of these attributes are shown in Table S2 in the ESM. These values were determined by taking an average of the trees' *DBH* and height within the given plot. The highest number of stems was recorded at 610 trees·ha^{-1} from plot 11, and the highest mean *DBH* (56.6 cm) and height (26.9 m) were recorded in plot 13, with the smallest number of stems being 90 trees·ha^{-1}. The lowest mean *DBH* and mean height were recorded at 18.38 cm, with the lowest mean height of 11.19 m.

Aboveground biomass and carbon stock estimation from inventory data of natural forest. The biomass estimation of natural forests includes aboveground biomass and carbon (Mg·ha^{-1}), belowground biomass (Mg·ha^{-1}), total biomass,

Table 3. Biomass and carbon stocks estimation of plot data in natural forest

Plot No.	*AGB*	*AGC*	*BGB*	*BGC*	Total biomass	Total C	CO_2e
				(Mg·ha^{-1})			
1	77.44	36.40	20.14	9.46	97.58	45.86	167.85
2	35.15	16.52	9.14	4.30	44.29	20.82	76.19
3	18.91	8.89	4.92	2.31	23.83	11.20	40.99
4	41.87	19.68	10.89	5.12	52.75	24.79	90.75
5	62.63	29.43	16.28	7.65	78.91	37.09	135.74
6	77.26	36.31	20.09	9.44	97.35	45.76	167.46
7	42.24	19.85	10.98	5.16	53.22	25.02	91.56
8	39.63	18.63	10.30	4.84	49.94	23.47	85.90
9	56.76	26.68	14.76	6.94	71.52	33.61	123.03
10	57.95	27.23	15.07	7.08	73.01	34.32	125.60
11	102.40	48.13	26.62	12.51	129.03	60.64	221.95
12	137.06	64.42	35.63	16.75	172.69	81.16	297.06
13	140.79	66.17	36.61	17.20	177.40	83.38	305.16
14	106.73	50.16	27.75	13.04	134.48	63.21	231.34
15	70.11	32.95	18.23	8.57	88.34	41.52	151.96
16	25.32	11.90	6.58	3.09	31.90	14.99	54.88
17	174.74	82.13	45.43	21.35	220.18	103.48	378.75
18	106.82	50.21	27.77	13.05	134.60	63.26	231.53
19	10.12	4.75	2.63	1.24	12.74	5.99	21.92
20	129.68	60.95	33.72	15.85	163.40	76.80	281.07
21	96.06	45.15	24.98	11.74	121.04	56.89	208.21
22	68.82	32.34	17.89	8.41	86.71	40.75	149.16
23	32.67	15.36	8.49	3.99	41.17	19.35	70.81
24	77.41	36.38	20.13	9.46	97.54	45.84	167.79
25	74.51	35.02	19.37	9.10	93.88	44.12	161.49
26	110.70	52.03	28.78	13.53	139.48	65.55	239.93
27	144.69	68.00	37.62	17.68	182.31	85.68	313.61
28	117.47	55.21	30.54	14.35	148.01	69.56	254.60
29	70.72	33.24	18.39	8.64	89.11	41.88	153.29

AGB – aboveground biomass; *BGB* – belowground biomass; *AGC* – aboveground carbon; *BGC* – belowground carbon

https://doi.org/10.17221/125/2022-JFS

and carbon stocks, as summarised in Table 3. The highest total biomass was 220.18 Mg·ha^{-1} with *AGB* and *BGB* of 174.74 Mg·ha^{-1} and 45.43 Mg·ha^{-1} in plot 17, whereas the lowest total biomass was 12.74 Mg·ha^{-1} in plot 19 with *AGB* and *BGB* 10.12 Mg·ha^{-1} and 2.63 Mg·ha^{-1}, respectively. The mean *AGB* and *BGB* were estimated as 79.54 Mg·ha^{-1} and 20.68 Mg·ha^{-1}, respectively, while the mean biomass for both *AGB* and *BGB* was 100.22 Mg·ha^{-1}, as presented in Table 3. Similarly, the highest total carbon stocks, *AGC* and *BGC*, were 103.48 Mg·ha^{-1}, 82.13 Mg·ha^{-1}, and 21.35 Mg·ha^{-1}, respectively, whereas the lowest total carbon stocks, *AGC*, and *BGC* were calculated as 5.99 Mg·ha^{-1}, 4.75 Mg·ha^{-1}, and 1.24 Mg·ha^{-1}, respectively. Regarding CO_2 equivalent, the highest (378.75 CO_2e) was found in plot 17, while the lowest 21.92 CO_2e was in plot 19. The mean *AGC* and *BGC* were 37.38 Mg·ha^{-1} and 9.72 Mg·ha^{-1}, respectively, whereas mean carbon stocks (including both *AGC* and *BGC*) were 47.10 Mg·ha^{-1}, as shown in Table 3.

Relationship between tree attributes and *AGB* of inventory data in natural forests. A simple linear regression model was developed between *AGB* (Mg·ha^{-1}) and plot-wise attributes (mean *DBH* and height). Results showed that mean *DBH* has a weak relationship with *AGB* and a correlation coefficient (R^2 = 0.46) with a polynomial model, which explained only 46% of data and 56% of *AGB* data remained unexplained (Figure 2A). The lower correlation of *DBH* versus *AGB* may be explained by the fact that plot-wise mean values were regressed against each other; if single tree measurements are correlated, the correlation coefficient would be better. Similarly, the mean height of each plot was regressed against plot-wise mean *AGB*, and the scatter plot showed that the correlation was lower (R^2 = 0.56) with the polynomial model (Figure 2B). This model explained only 56% of the *AGB*, whereas 44% of *AGB* data was left unexplained. However, its correlation was higher than the *DBH* polynomial model.

Sentinel-2 spectral indices for natural forests. Results of regression models between *AGB* (Mg·ha^{-1}) of *Pinus roxburghii* natural forest and Sentinel-2 spectral indices have been summarised in Table 4. All vegetation indices showed a strong relationship with field *AGB* data; Ratio Vegetation Index (*RVI*) showed the best performance with correlation (R^2 = 0.72), which means that the *RVI* polynomial model explained 72% of forest inventory data while the remaining 28% of *AGB* data remained unexplained (Figure 3C). Similarly, Normalized Difference Vegetation Index (*NDVI*) and Atmospherically Resistant Vegetation Index (*ARVI*) showed good performance, and the coefficient of correlation (R^2) was 0.70 for both indices (Figure 3A–B). It means that 70% of *AGB* was explained by *NDVI* and *ARVI* models, and the rest of the 30% data was not explained. *NDVI* has shown the highest correlation in the polynomial model, whereas *ARVI* achieved the highest correlation in the power model. Likewise, all indices showed that the distribution of *AGB* data was not the best fit with the linear regression model. Therefore, non-linear polynomial and power were best for *NDVI*, *RVI*, and *ARVI*, respectively (Table 4).

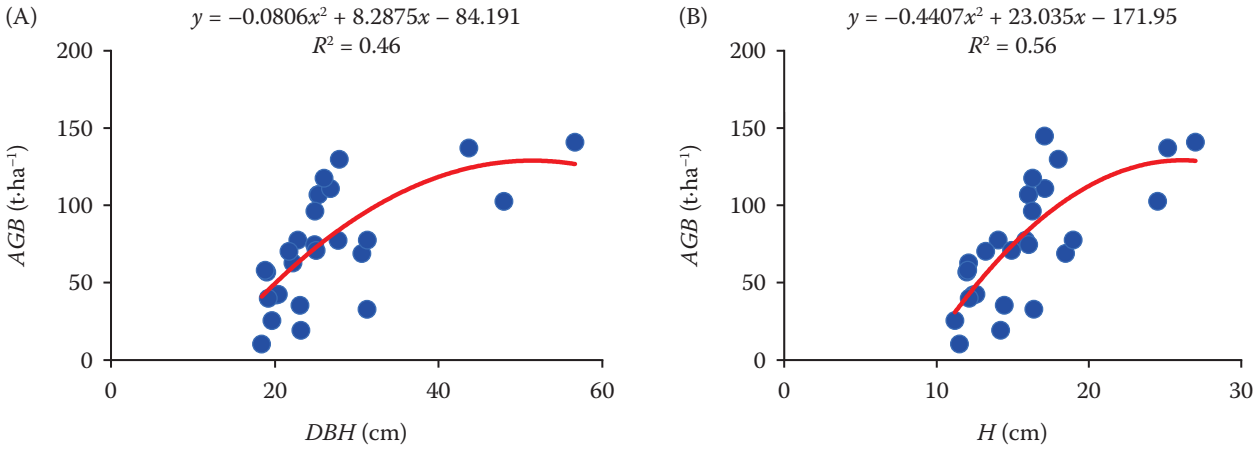

Figure 2. (A) *AGB* vs *DBH*; (B) *AGB* vs *H*

AGB – aboveground biomass; *DBH* – diameter at breast height; *H* – height

https://doi.org/10.17221/125/2022-JFS

Table 4. Summary of regression models between *AGB* and Sentinel-2 spectral indices

Index	Equation	Model	R^2
Natural forests			
NDVI	$y = -244.7x^2 + 614.48x - 154.23$	polynomial	0.70
ARVI	$y = 264.15x^{2.2769}$	power	0.70
RVI	$y = -11.452x^2 + 128.35x - 187.65$	polynomial	0.72
Plantations			
NDVI	$y = 5.7006e^{5.6445x}$	exponential	0.41
ARVI	$y = 13.029e^{3.1633x}$	exponential	0.40
RVI	$y = 8.7573x^{2.1666}$	power	0.41

AGB – aboveground biomass; *NDVI* – Normalized Difference Vegetation Index; *ARVI* – Atmospherically Resistant Vegetation Index; *RVI* – Ratio Vegetation Index

Hence, the polynomial model was used to minimise error and ensure best fit along the curvature of *AGB* data. The polynomial models of *NDVI* and *RVI* have shown a high correlation compared to linear models. However, their performance was affected by the data's outliers (Figures 3B–C). Similarly, in the case of *ARVI*, the correlation was increased using a power model, which means that

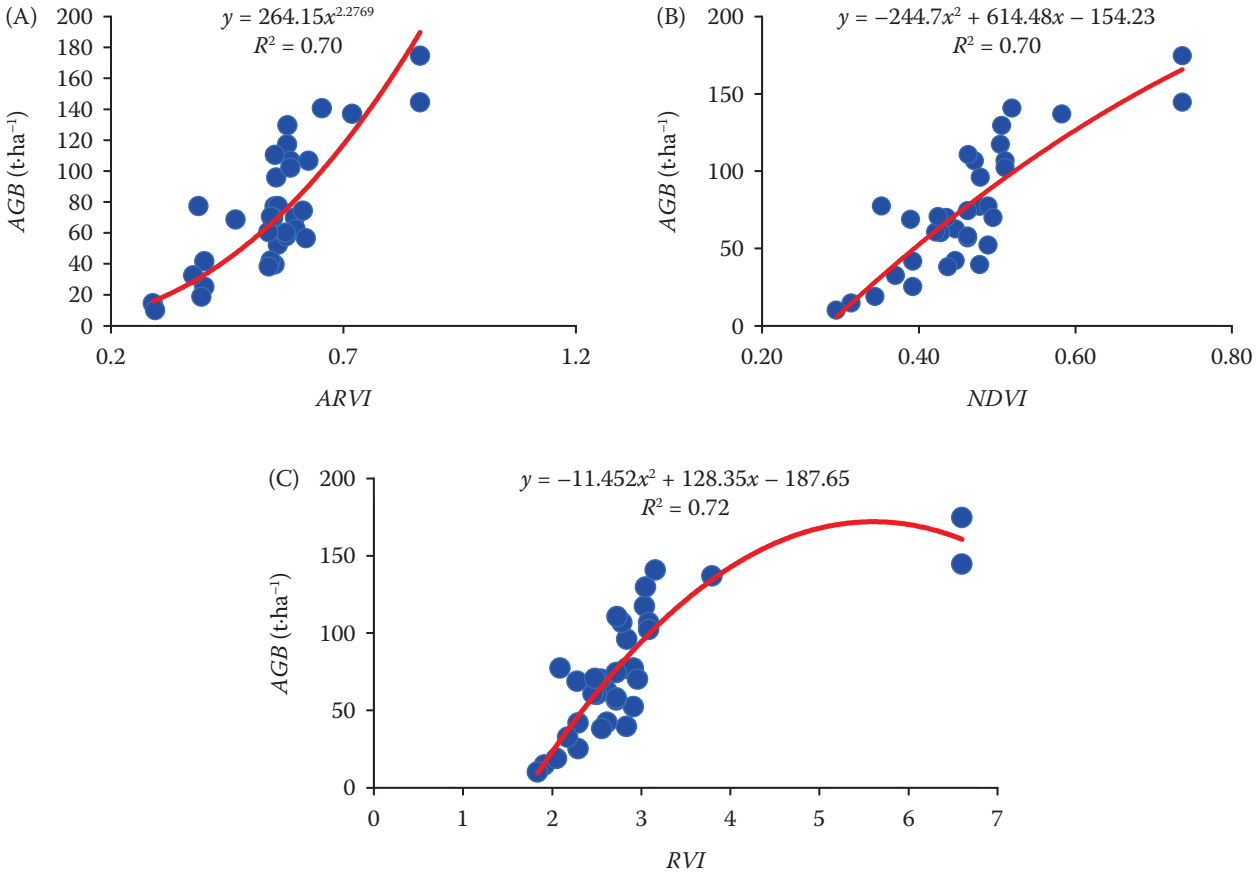

Figure 3. Relationships of Sentinel-2 vegetation indices and natural forest *AGB*; (A) *AGB* vs *ARVI*; (B) *AGB* vs *NDVI*; (C) *AGB* vs *RVI*

AGB – aboveground biomass; *ARVI* – Atmospherically Resistant Vegetation Index; *NDVI* – Normalized Difference Vegetation Index; *RVI* – Ratio Vegetation Index

https://doi.org/10.17221/125/2022-JFS

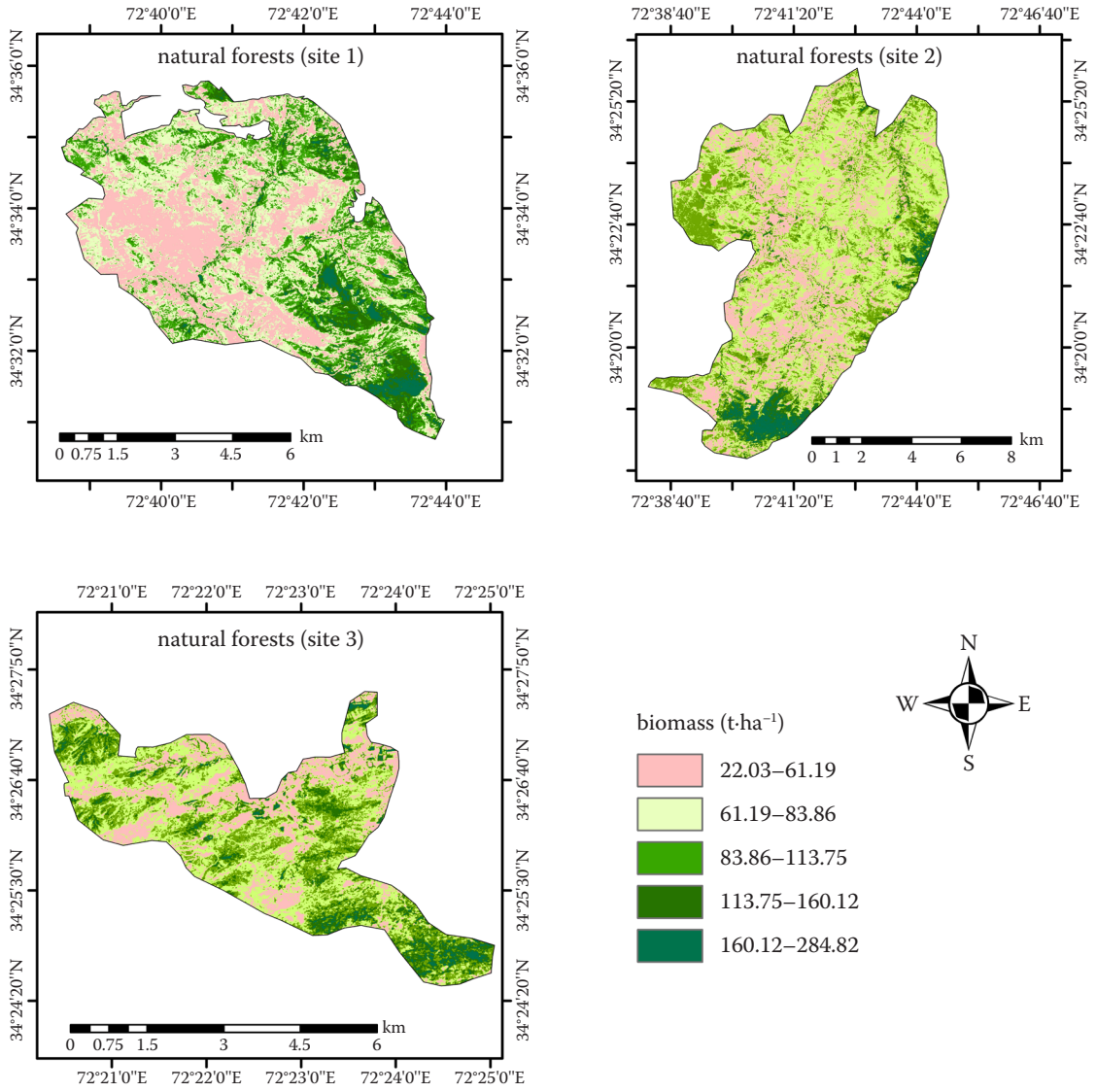

Figure 4. Biomass maps of different sites of natural forest in the study area

AGB data was proportional to *ARVI* values raised to a power. Comparatively, *RVI* was selected as the best index for *AGB* mapping of natural forests in the study area (Figure 4).

Tree attributes of plantation. The mean *DBH* and mean height of each plantation plot were determined, and the mean values of these attributes are shown in Table S3 in the ESM. The *DBH* and height mean values were calculated by averaging the *DBH* and height of the trees within the plot. The highest number of stems was recorded at 630 trees·ha^{-1} in plot 9. The highest mean *DBH* and height were 46 cm and 26.21 m, recorded in plot 17 with stem number (360 trees·ha^{-1}). The lowest mean *DBH* and mean height were recorded at 16 cm, with the lowest mean height of 10.43 m. Comparison of mean *DBH*, mean height and total biomass of natural forest and plantation have been represented in Figure 5.

Aboveground biomass and carbon stock estimation from inventory data of plantation. Plantation carbon stocks, aboveground biomass, belowground biomass (t·ha^{-1}), and total biomass and carbon stocks assessment is summarised in Table 5. According to Table 5, the highest total biomass was 360.05 Mg·ha^{-1} with *AGB* and *BGB* of 285.75 Mg·ha^{-1} and 74.30 Mg·ha^{-1} in plot 17. Likewise, the lowest total biomass is 28.26 Mg·ha^{-1}, with *AGB* and *BGB* 22.43 Mg·ha^{-1} and 5.83 Mg·ha^{-1} in plot 8, respectively. The mean *AGB* and *BGB* were

https://doi.org/10.17221/125/2022-JFS

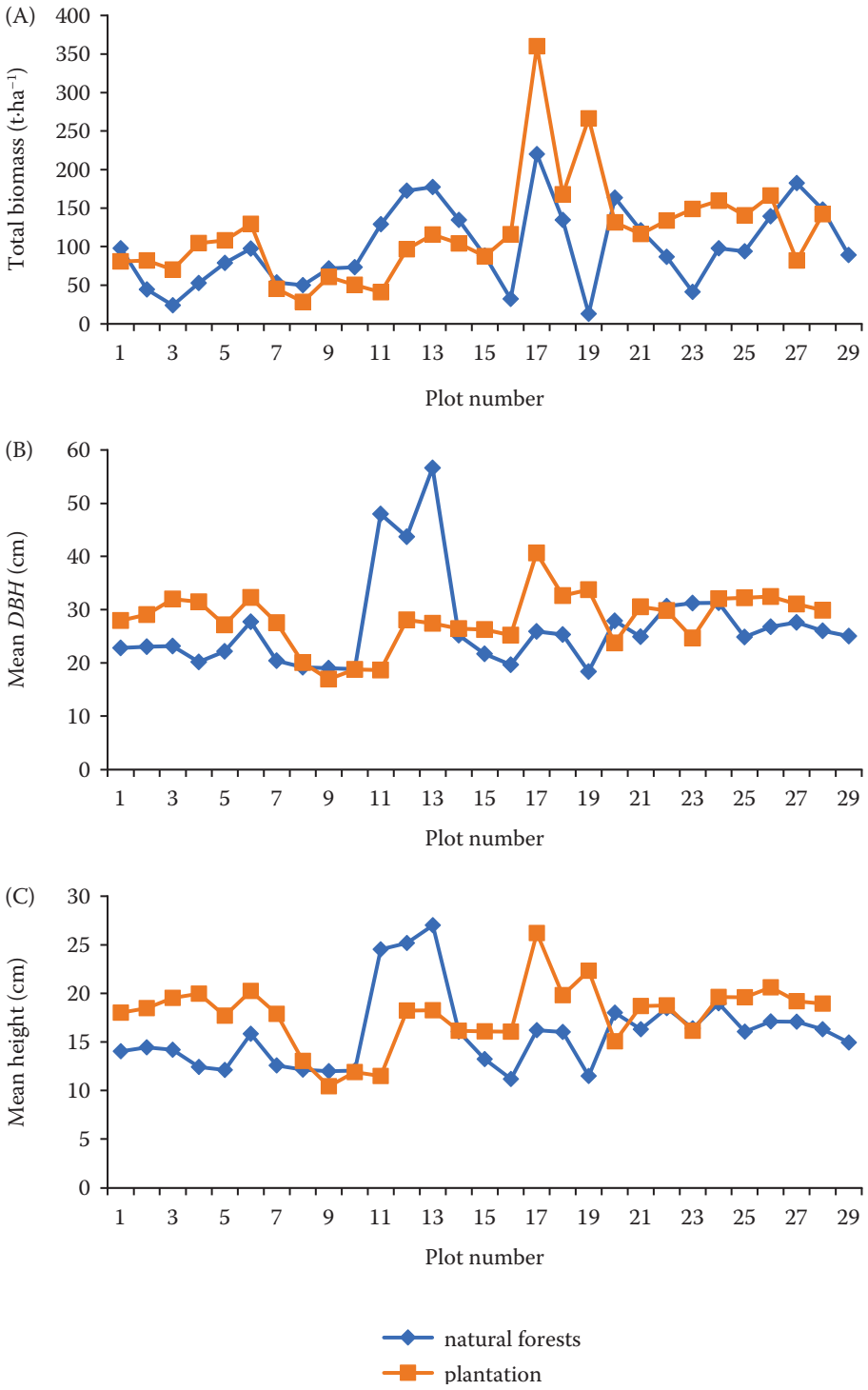

Figure 5. Comparison of mean *DBH*, mean height, and total biomass of natural forest and plantation

DBH – diameter at breast height

94.48 Mg·ha^{-1} and 24.56 Mg·ha^{-1}, respectively, whereas the mean biomass for both *AGB* and *BGB* was 119.04 Mg·ha^{-1}, as shown in Table 5. Concerning carbon stocks, the maximum total carbon stocks, *AGC* and *BGC*, were 169.22 Mg·ha^{-1}, 134.30 Mg·ha^{-1}, and 34.92 Mg·ha^{-1}, respectively, while the lowest total carbon stocks, *AGC* and *BGC*, were calculated as 13.28 Mg·ha^{-1}, 10.54 Mg·ha^{-1} and 2.74 Mg·ha^{-1}, respectively. Similarly, the highest CO_2 equivalent was 619.35 CO_2e

https://doi.org/10.17221/125/2022-JFS

Table 5. Biomass and carbon stock estimation of plot data in plantation

Plot No.	*AGB*	*AGC*	*BGB*	*BGC*	*TB*	*TC*	CO_2e
				(Mg·ha^{-1})			
1	63.93	30.05	16.62	7.81	80.55	37.86	138.57
2	65.14	30.62	16.94	7.96	82.08	38.58	141.20
3	55.46	26.06	14.42	6.78	69.88	32.84	120.19
4	82.80	38.92	21.53	10.12	104.33	49.03	179.45
5	85.82	40.34	22.31	10.49	108.14	50.82	186.00
6	102.63	48.24	26.68	12.54	129.32	60.78	222.45
7	35.82	16.83	9.31	4.38	45.13	21.21	77.63
8	22.43	10.54	5.83	2.74	28.26	13.28	48.60
9	48.04	22.58	12.49	5.87	60.53	28.45	104.13
10	39.78	18.70	10.34	4.86	50.13	23.56	86.23
11	32.38	15.22	8.42	3.96	40.80	19.18	70.20
12	76.50	35.95	19.89	9.35	96.39	45.30	165.80
13	91.56	43.03	23.81	11.19	115.37	54.22	198.45
14	82.70	38.87	21.50	10.11	104.20	48.98	179.27
15	69.33	32.58	18.02	8.47	87.35	41.05	150.24
16	92.16	43.32	23.96	11.26	116.12	54.58	199.76
17	285.75	134.30	74.30	34.92	360.05	169.22	619.35
18	133.30	62.65	34.66	16.29	167.95	78.94	288.92
19	211.23	99.28	54.92	25.81	266.15	125.09	457.83
20	104.25	49.00	27.10	12.74	131.35	61.73	225.93
21	92.30	43.38	24.00	11.28	116.29	54.66	200.06
22	106.05	49.84	27.57	12.96	133.62	62.80	229.85
23	118.23	55.57	30.74	14.45	148.96	70.01	256.24
24	126.46	59.44	32.88	15.45	159.34	74.89	274.10
25	111.62	52.46	29.02	13.64	140.64	66.10	241.93
26	131.93	62.01	34.30	16.12	166.23	78.13	285.96
27	64.94	30.52	16.88	7.94	81.82	38.46	140.76
28	112.88	53.05	29.35	13.79	142.23	66.85	244.67
Mean	94.48	44.41	24.56	11.55	119.04	55.95	204.78

AGB – aboveground biomass; *AGC* – aboveground carbon; *BGB* – belowground biomass; *BGC* – belowground carbon; *TB* – total biomass; *TC* – total carbon

in plot 17, while the lowest 48.60 CO_2e was in plot 8. As shown in Table 5, the mean *AGC* and *BGC* were 44.41 Mg·ha^{-1} and 11.55 Mg·ha^{-1}, respectively, but the mean carbon stocks (containing both *AGC* and *BGC*) were 55.95 Mg·ha^{-1}.

Sentinel-2 spectral indices for plantation. Results of regression models between *AGB* (Mg·ha^{-1}) of *Pinus roxburghii* plantation and Sentinel-2 spectral indices have been summarised in Table 4. All vegetation indices were good with field *AGB* data. However, *RVI* represents the strongest correlation (R^2 = 0.41). The *RVI* power model represented 41% of the forest inventory data model, while the other 59% of *AGB* data remained unexplained (Figure 6B). Similarly, *NDVI* also showed good performance with the correlation coefficient (R^2 = 0.41), as shown in Figure 6A. *ARVI* performed the lowest correlation with an R^2 of 0.40, which means that the *ARVI* model explained only 40% of *AGB*, and the remaining 60% of the data was not

https://doi.org/10.17221/125/2022-JFS

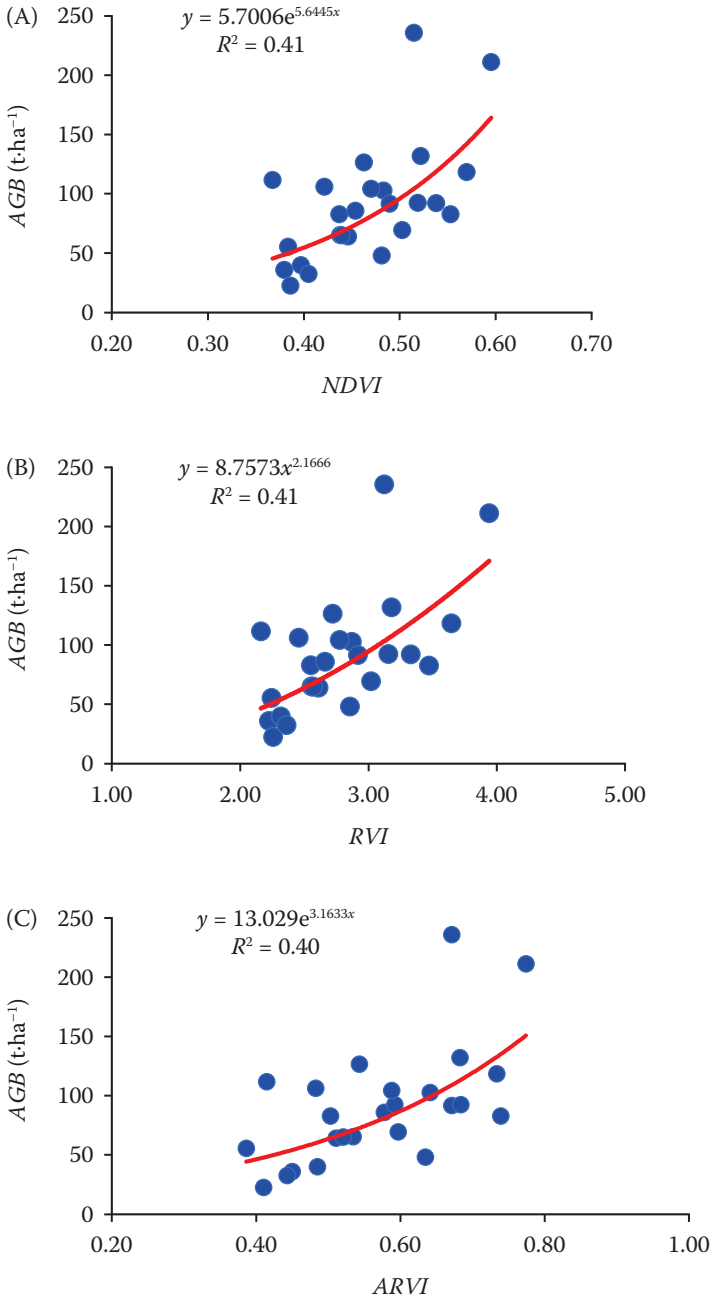

Figure 6. Scatterplots of Sentinel-2 vegetation indices and plantation *AGB*; (A) *AGB* vs *NDVI*; (B) *AGB* vs *RVI*; (C) *AGB* vs *ARVI*

AGB – aboveground biomass; *NDVI* – Normalized Difference Vegetation Index; *RVI* – Ratio Vegetation Index; *ARVI* – Atmospherically Resistant Vegetation Index

defined (Figure 6C). All indices showed that the distribution of *AGB* data was not the best fit with the linear regression model. Therefore, non-linear exponential and power were best for *NDVI*, *RVI*, and *ARVI*, respectively (Table 4). Linear regression showed less correlation and high error or cost function. Therefore, non-linear models (exponential and power) were used to minimise error and ensure best fit along the curvature of *AGB* data. Similarly, *RVI* correlation was increased using the power model, which means that *AGB* data was proportional to *RVI* values raised to a power. On the other hand, the exponential models of *NDVI* and *ARVI* have shown a high correlation compared to linear models. *RVI*-based model was used for *AGB* mapping in plantation sites of the study area (Figure 7).

https://doi.org/10.17221/125/2022-JFS

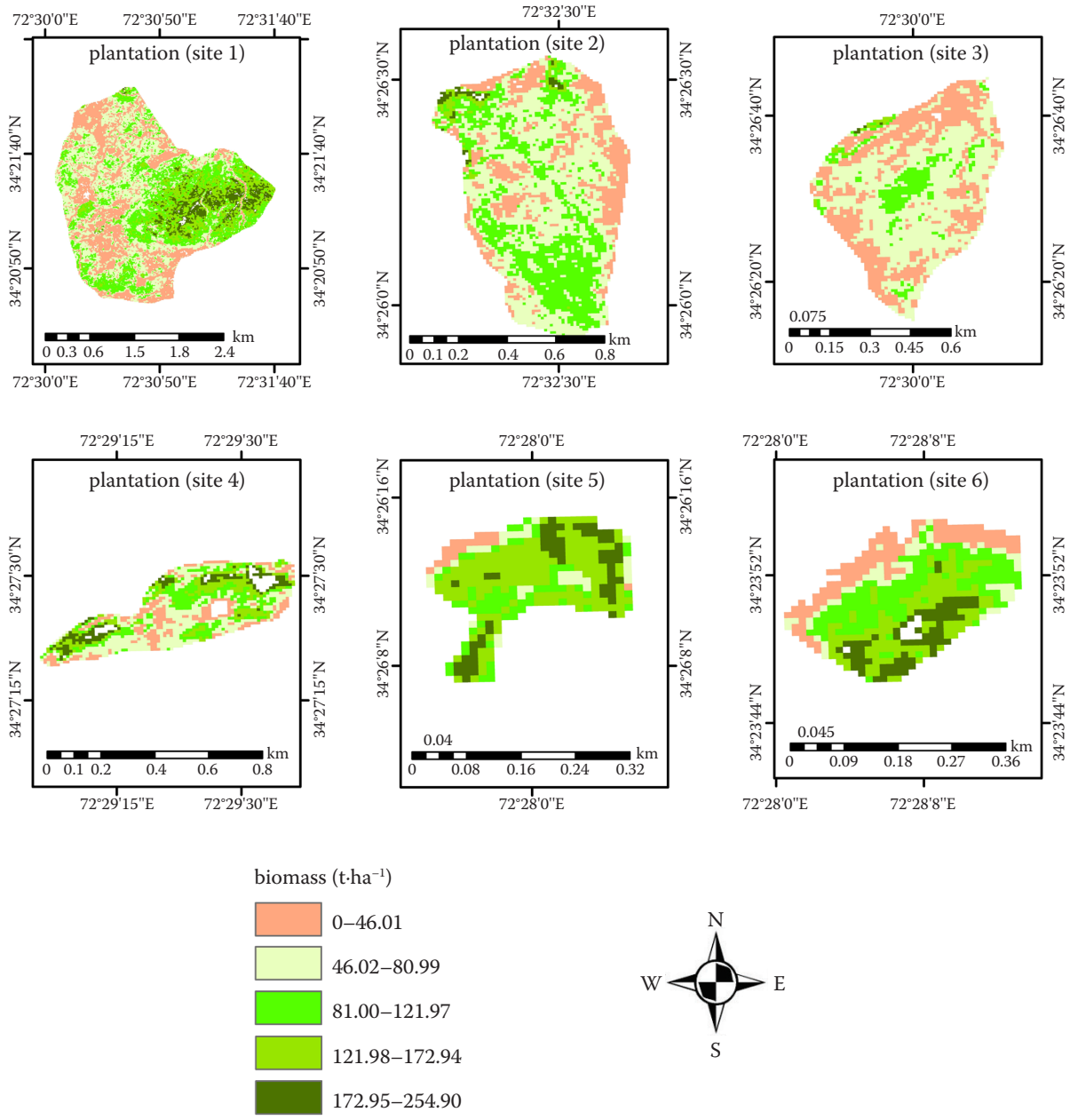

Figure 7. Biomass maps of different sites of plantation in the study area

DISCUSSION

***AGB* and carbon stock estimation.** In the present research, the average number was 302 trees·ha^{-1} in the natural forest. In comparison, in artificial plantations, the average number was 326 trees·ha^{-1}, similar to 332 trees·ha^{-1} for conifer forests of Mansehra, Pakistan (Ali et al. 2017). At the same time, Nizami et al. (2009) reported an average of 211 chir pine trees·ha^{-1} having greater than 21 cm diameter in Ghoragali. In another area, however, a smaller number of trees per hectare (149 trees·ha^{-1}) with the same stem diameter (21 cm) was found (Lehterar). Likewise, the over-matured chir pine stand has less density (147 trees·ha^{-1}) compared to the young pine stand (with 636 trees·ha^{-1}) in the Ghoragali forest managed under the shelterwood silvicultural system (Amir et al. 2018). Ali et al. (2020a) reported that the *DBH* and height of the sampled trees ranged from 12 cm to 93 cm and 9.50 m to 40.10 m, respectively. Sheikh et al. (2012) estimated that the average *DBH* was 34.80 cm and the average height was 17.24 m, with a stand density of 275 trees·ha^{-1}. Nizami et al. (2009)

https://doi.org/10.17221/125/2022-JFS

reported maximum height (31 m) and maximum *DBH* (64 cm) in a natural forest of *Pinus roxburghii*. According to Shaheen et al. (2016), tree density was 492 trees·ha^{-1}, with an average *DBH* of 87.27 cm and a tree height of 13.3 m. However, the current study tree density is lower than the reported tree density of the Indian chir pine forest (Pant, Tewari 2020), possibly due to age difference and other external disturbances because the local community depends on these forests for fuel and construction wood collection, resulting in forest degradation.

The presented study compared different tree attributes such as diameter at breast height and height of chir pine plantation and natural forest. Furthermore, the study comparatively examined the aboveground biomass of planted and natural chir pine forests. The results showed that plantations store more carbon than natural forests because the mean *DBH* and height of plantations were greater than those of natural forests. Several studies found a high link between *DBH* and biomass, height and biomass (Banday et al. 2018), and no relationship between tree density and carbon stock (Sharma et al. 2020). In the present study, the aboveground biomass is comparatively lower than that of the chir pine plantation in India, reported as 154.33 Mg·ha^{-1} (Bandy et al. 2018). Another study in the Indian chir pine forest reported that aboveground biomass ranged from 97 Mg·ha^{-1} to 145 Mg·ha^{-1} (Pant, Tewari 2020). Amir et al. (2018) estimated tree biomass and carbon stocks of young, mature, and over-matured chir pine trees, and the results showed that the highest biomass was 529 Mg·ha^{-1} for over-matured trees, followed by the 343 Mg·ha^{-1} for mature stands and 80 Mg·ha^{-1} for young trees. Similarly, carbon contents were 264 Mg·ha^{-1}, 172 Mg·ha^{-1}, and 40 Mg·ha^{-1} for over-matured, mature, and young chir pine trees, respectively. Ali et al. (2018) reported that *AGB* in the mixed forest was 149 Mg·ha^{-1} with 39 Mg·ha^{-1} of biomass in the underground parts of vegetation. The study reported total carbon contents (88 Mg·ha^{-1}), in which 70 Mg·ha^{-1} carbon contents in aboveground vegetation and 18 Mg·ha^{-1} in belowground parts in subtropical scrub forests in Haripur, Pakistan. To accurately estimate biomass, local developed allometric equation is used. However, the literature review indicated that there is no allometric equation available for chir pine of our study area. A recent review also stated that there is a lack of local developed allometric equation for major species (Khan et al. 2021a).

Chir pine species is one of the notable coniferous species in the study area and has the potential to sequester more carbon, keeping in view the protection and conservation of chirpine forests (Ali et al. 2020b). The chirpine forests are of great significance in the context of GCC as these species have a long rotation period and can fix a huge amount of carbon from the atmosphere.

Vegetation indices and *AGB* estimation. The research results were also consistent with Pandit et al. (2018), who estimated the *AGB* of forests and reported *NDVI* with correlation (R^2 = 0.70). However, this study also computed red-edge band-based *NDVI*, which showed an R^2 of 0.80 (Pandit et al. 2018). Similarly, Imran and Ahmed (2018) also estimated *AGB* in subtropical pine forests using spectral indices (*NDVI* and *ARVI*). This study reported that *NDVI* performed better with the correlation (R^2 = 0.67), whereas *ARVI* performance was not impressed with correlation (R^2 = 0.23). In another study, Imran et al. (2020) explored various broadband and narrowband indices computed from Sentinel-2 and reported *NDVI* and *ARVI* to estimate *AGB*. This study also said that *NDVI* performed better than *ARVI* and showed a correlation coefficient of 0.53 and 0.31, respectively. Many other recent studies reported a high correlation for *NDVI*, such as Shaheen et al. (2016), which showed an R^2 of 0.80, and Adan (2017), which showed an R^2 of 0.60. Like *NDVI*, *RVI* was also reported to be an efficient vegetation index for *AGB* and carbon stock estimation (Das, Singh 2012; Kumar, Shekhar 2015). Similarly, recent research also used Sentinel-2 spectral indices to estimate *AGB* in moist temperate forests and reported a lower correlation (R^2 = 0.28) for *NDVI* (Khan et al. 2020). Das and Singh (2012) assessed the relationship of vegetation indices against *AGB* and concluded that *RVI* showed the best performance with an R^2 of 0.78, followed by *NDVI* with an R^2 of 0.75. Nuthammachot et al. (2018) used Sentinel-2 indices to estimate *AGB* in private forests and reported 0.80 and 0.85 correlations for *NDVI* and simple ratio, respectively. Therefore, a simple ratio may outperform *NDVI* in predicting the biophysical properties of vegetation (Frampton et al. 2013). Furthermore, many kinds of research showed that broadband vegetation indices experienced saturation issues in high forest density, resulting in a lower correlation of *NDVI* with biomass (Imran et al. 2020; Khan et al. 2020). Similarly, Steininger (2000) and

https://doi.org/10.17221/125/2022-JFS

Kasischke et al. (2014) reported that the accuracy of predicated *AGB* is significantly affected by vegetation indices saturation in dense forests (stocking density from 80 to 100). This may be caused by the fact that the reflectance might diffuse within dense canopy cover, thus distorting the actual signal. Vafaei et al. (2018) explored Sentinel-2 images combined with PALSAR-2 to estimate biomass and indicated that integrating optical and radar images significantly improved biomass prediction. The study used *NDVI* and *RVI* to model biomass. However, Sentinel-2 performed better (high correlation) than PALSAR-2. Vegetation mapping and modelling from local or regional to large continental scales was performed with vegetation indices (Wang et al. 2004; Wessels et al. 2004; Amiri, Tabatabaie 2009). In the context of temporal changes in vegetation, such as seasonal or annual variations and comparison, NDVI provides meaningful derived information to identify vegetation health and stress conditions (Chen et al. 2006; Zoran, Stefan 2006).

CONCLUSION

This research study investigated carbon stock in two pools, *AGB* and *BGB*, in the chir pine natural forests and in chir pine plantations of Buner District. Results showed that the highest mean *DBH* and height in natural forests were 56.6 cm and 26.9 m, while the lowest mean *DBH* and mean height were recorded at 18.38 cm, with the lowest mean height of 11.19 m. Similarly, the highest total biomass was 220.18 Mg·ha^{-1} with *AGB* and *BGB* of 174.74 Mg·ha^{-1} and 45.43 Mg·ha^{-1} in plot 17, whereas the lowest total biomass was 12.74 Mg·ha^{-1} in plot 19 with *AGB* and *BGB* 10.12 Mg·ha^{-1} and 2.63 Mg·ha^{-1}, respectively. On the other hand, concerning the plantation, the highest mean *DBH* and height were 46 cm and 26.21 m, whereas the lowest mean *DBH* and mean height were recorded at 16 cm with the lowest mean height, 10.43 m. Similarly, the plantation's highest total biomass was 360.05 Mg·ha^{-1}, with *AGB* and *BGB* of 285.75 Mg·ha^{-1} and 74.30 Mg·ha^{-1}, respectively. The plantation's lowest total biomass was 28.26 Mg·ha^{-1}, with *AGB* and *BGB* at 22.43 Mg·ha^{-1} and 5.83 Mg·ha^{-1}, respectively. It would be beneficial to implement this study's results in forest management practices. Also, the development of this study would be helpful in the debate on carbon storage in managed and natural forests.

Furthermore, the present study could also be helpful in forest management to increase carbon sequestration. Exploring Sentinel-2 in Pakistan, specifically in the study area, will provide a pilot study for future research and contribute to regional carbon stocks and emission accounting. LiDAR canopy height, combined with other remote sensing techniques, has proved to be successful at demonstrating estimates of aboveground biomass (*AGB*) with high accuracy levels. Nandy et al. (2021) used a random forest algorithm to interpolate canopy height from a combination of spectral variables obtained from Sentinel-2 and ICESat-2 data, resulting in improved estimates of forest height and *AGB* in subtropical forests. Modelling accurate *AGB* in mountainous regions with diverse topography is always a challenging task. The present study utilised Sentinel-2 spectral indices to model *AGB*, but the accuracy of this approach can be further improved by incorporating LiDAR data (Narine et al. 2019; Chen et al. 2022). The fusion of pixel-sized LiDAR data and *AGB* spectral predictors can significantly reduce landscape heterogeneity and *AGB* saturation. However, acquiring ubiquitous coverage of LiDAR data for large-scale *AGB* estimation can be costly and commercially challenging (Su et al. 2020). In Pakistan, the use of LiDAR systems is currently limited to smaller areas, and thus a LiDAR-based analysis for *AGB* modelling was not considered due to its high cost and limited acquisition scope. The present study has several limitations that may affect the accuracy of *AGB* estimation. One of the limitations is the use of third-party allometric equations, which may not account for local variations within the stand. Developing locally-based standard allometric equations is crucial for accurately estimating *AGB*. Additionally, variations of biomass in dense canopies in subtropical forests may not be accurately quantified by Sentinel-2 images with a spatial resolution of 10 metres. The research concluded that forests of the study area have a great potential for conservation projects such as Reducing Emissions from Deforestation and Forest Degradation (REDD+). If the REDD+ project and forest management under REDD+ are implemented in the study area, it will positively impact the forest cover, local communities, and other stakeholders. Moreover, the study suggests that the accuracy of carbon stock estimates can be enhanced by using locally developed allometric equations and high-resolution remote sensing data.

https://doi.org/10.17221/125/2022-JFS

REFERENCES

Adan M.S. (2017): Integrating Sentinel-2 derived vegetation indices and terrestrial laser scanner to estimate above-ground biomass/carbon in Ayer Hitam tropical forest Malaysia. [MSc. Thesis.] Enschede, University of Twente.

Afzal M., Akhtar A.M. (2011): Estimation of biomass and carbon stock: Chichawatni Irrigated Plantation in Punjab, Pakistan. In: SDPI's 14th Sustainable Development Conference, Islamabad, Dec 13–15, 2011.

Ahmad N., Ullah S., Zhao N., Mumtaz F., Ali A., Ali A., Shakir M. (2023): Comparative analysis of remote sensing and geo-statistical techniques to quantify forest biomass. Forests, 14: 379.

Ali A., Ayaz M., Muhammad S. (2017): A study of stand structure of temperate forests of Kaghan valley, Mansehra, Khyber Pakhtunkhwa. The Pakistan Journal of Forestry, 67: 20171.

Ali A., Saleem U., Shaiza B., Naveed A., Asad A., Khan M.A. (2018): Quantifying forest carbon stocks by integrating satellite images and forest inventory data. Austrian Journal of Forest Science/Centralblatt für das gesamte Forstwesen, 135: 93–117.

Ali A., Ashraf M.I., Gulzar S., Akmal M. (2020a): Development of an allometric model for biomass estimation of *Pinus roxburghii*, growing in subtropical pine forests of Khyber Pakhtunkhwa, Pakistan. Sarhad Journal of Agriculture, 36: 236–244.

Ali A., Ashraf M.I., Gulzar S., Akmal M. (2020b): Estimation of forest carbon stocks in temperate and subtropical mountain systems of Pakistan: implications for REDD+ and climate change mitigation. Environmental Monitoring and Assessment, 192: 1–13.

Amir M., Liu X., Ahmad A., Saeed S., Mannan A., Muneer M.A. (2018): Patterns of biomass and carbon allocation across chronosequence of chir pine (*Pinus roxburghii*) forest in Pakistan: Inventory-based estimate. Advances in Meteorology, 2018: 1–8.

Amiri F., Tabatabaie T. (2009): Operational monitoring of vegetative cover by remote sensing in semi-arid lands of Iran. In: Proceedings of the 7th FIG Regional Conference, Spatial Data Serving People: Land Governance and the Environment-Building the Capacity, Hanoi, Oct 19–22, 2009: 1–18.

Babbar D., Areendran G., Sahana M., Sarma K., Raj K., Sivadas A. (2021): Assessment and prediction of carbon sequestration using Markov chain and InVEST model in Sariska Tiger Reserve, India. Journal of Cleaner Production, 278: 123333.

Banday M., Bhardwaj D.R., Pala N.A. (2018): Variation of stem density and vegetation carbon pool in subtropical forests of Northwestern Himalaya. Journal of Sustainable Forestry, 37: 389–402.

Bukhari B.S.S., Haider A., Laeeq M.T. (2012): LAND Cover Atlas of Pakistan. Peshawar, Pakistan Forest Institute: 140.

Castillo J.A.A., Apan A.A., Maraseni T.N.., Salmo S.G. (2017): Estimation and mapping of above-ground biomass of mangrove forests and their replacement land uses in the Philippines using Sentinel imagery. ISPRS Journal of Photo and Remote Sensing, 134: 75–85.

Chen P.Y., Fedosejevs G., Tiscareño-López M., Arnold J.G. (2006): Assessment of MODIS-EVI, MODIS-NDVI and VEGETATION-NDVI composite data using agricultural measurements: An example at corn fields in western Mexico. Environmental Monitoring and Assessment, 119: 69–82.

Chen L., Ren C., Bao G., Zhang B., Wang Z., Liu M., Liu J. (2022): Improved object-based estimation of forest above-ground biomass by integrating LiDAR data from GEDI and ICESat-2 with multi-sensor images in a heterogeneous mountainous region. Remote Sensing, 14: 2743.

Das S., Singh T.P. (2012): Correlation analysis between biomass and spectral vegetation indices of forest ecosystem. International Journal of Engineering Research & Technology, 1: 1–13.

FAO (2020): Global Forest Resources Assessment 2020 – Key Findings. Rome, FAO: 16.

Frampton W.J., Dash J., Watmough G., Milton E.J. (2013): Evaluating the capabilities of Sentinel-2 for quantitative estimation of biophysical variables in vegetation. ISPRS Journal of Photogrammetry and Remote Sensing, 82: 83–92.

Goetz S., Dubayah R. (2011): Advances in remote sensing technology and implications for measuring and monitoring forest carbon stocks and change. Carbon Management, 2: 231–244.

Houghton R.A., Byers B., Nassikas A.A. (2015). A role for tropical forests in stabilizing atmospheric CO_2. Nature Climate Change, 5: 1022–1023.

Huang L., Zhou M., Lv J., Chen K. (2020): Trends in global research in forest carbon sequestration: A bibliometric analysis. Journal of Cleaner Production, 252: 119908.

Imran A.B., Ahmed S. (2018): Potential of Landsat-8 spectral indices to estimate forest biomass. International Journal of Human Capital in Urban Management, 3: 303–314.

Imran A.B., Khan K., Ali N., Ahmad N., Ali A., Shah K. (2020): Narrow band based and broadband derived vegetation indices using Sentinel-2 Imagery to estimate vegetation biomass. Global Journal of Environmental Science and Management, 6: 97–108.

Isbaex C., Coelho A.M. (2021): The potential of Sentinel-2 satellite images for land-cover/land-use and forest biomass estimation: A review. In: Forest Biomass: From Trees to Energy. London, IntechOpen: 1–24.

https://doi.org/10.17221/125/2022-JFS

Jallat H., Khokhar M.F., Kudus K.A., Nazre M., Saqib N.U., Tahir U., Khan W.R. (2021): Monitoring carbon stock and land-use change in 5000-year-old juniper forest stand of ziarat, Balochistan, through a synergistic approach. Forests, 12: 1–15.

Kasischke E.S., Kane E.S., Genet H., Turetsky M.R., O'Donnell J.A., Hoy E., Barrett K., Baltzer J.L. (2014): A geographic perspective on factors controlling post-fire succession in boreal black spruce forests in Western North America. In: AGU Fall Meeting Abstracts, San Francisco, Dec 15–19, 2014: B31D-0038.

Kaufman Y.J., Tanre D. (1992): Atmospherically resistant vegetation index (ARVI) for EOS-MODIS. IEEE Transactions on Geoscience and Remote Sensing, 30: 261–270.

Khan K., Iqbal J., Ali A., Khan S.N. (2020): Assessment of Sentinel-2-derived vegetation indices for the estimation of aboveground biomass/carbon stock, temporal deforestation and carbon emissions estimation in the moist temperate forests of Pakistan. Applied Ecology and Environmental Research, 18: 783–815.

Khan I.A., Khan W.R., Ali A., Nazre M. (2021a): Assessment of above-ground biomass in Pakistan forest ecosystem's carbon pool: A review. Forests, 12: 586.

Khan R.W.A., Shaheen H., Awan S.N. (2021b): Biomass and soil carbon stocks in relation to the structure and composition of chir Pine dominated forests in the lesser Himalayan foothills of Kashmir. Carbon Management, 12: 429–437.

Khati U., Singh G., Ferro-Famil L. (2017): Analysis of seasonal effects on forest parameter estimation of Indian deciduous forest using TerraSAR-X PolInSAR acquisitions. Remote Sensing Environment, 199: 265–276.

Kumar D., Shekhar S. (2015): Statistical analysis of land surface temperature–vegetation indexes relationship through thermal remote sensing. Ecotoxicology and Environmental Safety, 121: 39–44.

Kumar L., Mutanga O. (2017): Remote sensing of aboveground biomass. Remote Sensing, 9: 935.

Kyere-Boateng R., Marek M.V. (2021): Analysis of the social-ecological causes of deforestation and forest degradation in Ghana: Application of the DPSIR framework. Forests, 12: 409.

Lamlom S., Savidge R. (2003): A reassessment of carbon content in wood: variation within and between 41 North American species. Biomass and Bioenergy, 25: 381–388.

Malhi Y., Baker T.R., Phillips O.L., Almeida S., Alvarez E., Arroyo L., Chave J., Czimczik C.I., Di Fiore A., Higuchi N., Killeen T.J., Laurance S.G., Laurance W.F., Lewis S.L., Montoya L.M.M., Monteaguda A., Neill D.A., Vargas P.N., Patiño S., Pitman N.A.C., Quesada C.A., Salomão R., Silva J.N.M., Lezama A.T., Martínez R.V., Terborgh J., Vinceti B., Lloyd J. (2004): The aboveground coarse wood productivity of 104 Neotropical forest plots. Global Change Biology, 10: 563–591.

Musthafa M., Singh G. (2022): Improving forest aboveground biomass retrieval using multi-sensor L-and C-Band SAR data and multi-temporal spaceborne LiDAR data. Frontiers in Forests and Global Change, 5: 14.

Musthafa M., Khati U., Singh G. (2020): Sensitivity of PolSAR decomposition to forest disturbance and regrowth dynamics in a managed forest. Advances in Space Research, 66: 1863–1875.

Narine L.L., Popescu S., Neuenschwander A., Zhou T., Srinivasan S., Harbeck K. (2019): Estimating aboveground biomass and forest canopy cover with simulated ICESat-2 data. Remote Sensing of Environment, 224: 1–11.

Nhangumbe M., Nascetti A., Ban Y. (2023): Multi-Temporal Sentinel-1 SAR and Sentinel-2 MSI Data for Flood Mapping and Damage Assessment in Mozambique. ISPRS International Journal of Geo-Information, 12: 53.

Nizami S.M. (2012): The inventory of the carbon stocks in sub tropical forests of Pakistan for reporting under Kyoto Protocol. Journal of Forestry Research, 23: 377–384.

Nizami S.M., Mirza S.N., Livesley S., Arndt S., Fox J.C., Khan I.A., Mahmood T. (2009): Estimating carbon stocks in sub-tropical pine (*Pinus roxburghii*) forests of Pakistan. Pakistan Journal of Agricultural Sciences, 46: 266–270.

Nuthammachot N., Phairuang W., Wicaksono P., Sayektiningsih T. (2018): Estimating aboveground biomass on private forest using Sentinel-2 imagery. Journal of Sensors, 2018: 1–11.

Nyamari N., Cabral P. (2021): Impact of land cover changes on carbon stock trends in Kenya for spatial implementation of REDD+ policy. Applied Geography, 133: 102479.

Pandit S., Tsuyuki S., Dube T. (2018): Estimating aboveground biomass in sub-tropical buffer zone community forests, Nepal, using Sentinel 2 data. Remote Sensing, 10: 601.

Pant H., Tewari A. (2020): Green sequestration potential of chir pine forests located in Kumaun Himalaya. Forest Products Journal, 70: 64–71.

Pearson T.R.H., Brown S.L., Birdsey R.A. (2007): Measurement Guidelines for the Sequestration of Forest Carbon. Vol. 18. Newtown Square, US Department of Agriculture, Forest Service, Northern Research Station: 42.

Qureshi A., Badola R., Hussain S.A. (2012): A review of protocols used for assessment of carbon stock in forested landscapes. Environmental Science & Policy, 16: 81–89.

Rahman S.U., Ullah Z., Ali A., Ahmad M., Sher H., Shinwari Z.K., Nazir A. (2022): Ethnoecological knowledge of wild fodder plant resources of district buner Pakistan. Pakistan Journal of Botany, 54: 645–652.

Raihan A., Begum R.A., Mohd Said M.N., Abdullah S.M.S. (2019): A review of emission reduction potential and cost

https://doi.org/10.17221/125/2022-JFS

savings through forest carbon sequestration. Asian Journal of Water, Environment and Pollution, 16: 1–7.

Ravindranath N.H., Ostwald M. (2008): Methods for estimating aboveground biomass. In: Carbon Inventory Methods. Handbook for Greenhouse Gas Inventory, Carbon Mitigation and Roundwood Production Projects. Dordrecht, Springer: 113–147.

Rouse J.W., Haas R.H., Schell J.A., Deering D.W. (1973): Monitoring vegetation systems in the Great Plains with ERTS. Available at: https://ntrs.nasa.gov/api/citations/19740022614/downloads/19740022614.pdf.

Satyal P., Paudel P., Raut J., Deo A., Dosoky N.S., Setzer W.N. (2013): Volatile constituents of *Pinus roxburghii* from Nepal. Pharmacognosy Research, 5: 43–48.

Seidel D., Fleck S., Leuschner C., Hammett T. (2011): Review of ground-based methods to measure the distribution of biomass in forest canopies. Annals of Forest Science, 68: 225–244.

Shaheen H., Khan R.W.A., Hussain K., Ullah T.S., Nasir M., Mehmood A. (2016): Carbon stocks assessment in subtropical forest types of Kashmir Himalayas. Pakistan Journal of Botany, 48: 2351–2357.

Sharma K.P., Bhatta S.P., Khatri G.B., Pajiyar A., Joshi D.K. (2020): Estimation of carbon stock in the chir pine (*Pinus roxburghii Sarg.*) plantation forest of Kathmandu Valley, Central Nepal. Journal of Forest and Environmental Science, 36: 37–46.

Sheikh M.A., Kumar S., Kumar M. (2012): Above and below ground organic carbon stocks in a sub-tropical *Pinus roxburghii* Sargent forest of the Garhwal Himalayas. Forestry Studies in China, 14: 205–209.

Shoko C., Mutanga O. (2017): Examining the strength of the newly-launched Sentinel 2 MSI sensor in detecting and discriminating subtle differences between C3 and C4 grass species. ISPRS Journal of Photogrammetry and Remote Sensing, 129: 32–40.

Siddiq Z., Hayyat M.U., Khan A.U., Mahmood R., Shahzad L., Ghaffar R., Cao K.F. (2021): Models to estimate the above and below ground carbon stocks from a subtropical scrub forest of Pakistan. Global Ecology and Conservation, 27: e01539.

Steininger M. (2000): Satellite estimation of tropical secondary forest aboveground biomass: Data from Brazil and Bolivia. International Journal of Remote Sensing, 21: 1139–1157.

Su H., Shen W., Wang J., Ali A., Li M. (2020): Machine learning and geostatistical approaches for estimating aboveground biomass in Chinese subtropical forests. Forest Ecosystems, 7: 64.

Sun X., Guicai L., Meng W., Zemeng F. (2019): Analyzing the uncertainty of estimating forest aboveground biomass using optical imagery and space-borne LiDAR. Remote Sensing, 11: 722.

Thammanu S., Han H., Marod D., Srichaichana J., Chung J. (2021): Aboveground carbon stock and REDD+ opportunities of community-managed forests in northern Thailand. PLoS ONE, 16: e0256005.

Tucker C.J. (1979): Red and photographic infrared linear combinations for monitoring vegetation. Remote Sensing of Environment, 8: 127–150.

Vafaei S., Soosani J., Adeli K., Fadaei H., Naghavi H., Pham T.D., Tien Bui D. (2018): Improving accuracy estimation of Forest Aboveground Biomass based on incorporation of ALOS-2 PALSAR-2 and Sentinel-2A imagery and machine learning: A case study of the Hyrcanian forest area (Iran). Remote Sensing, 10: 172.

Wang Y., Woodcock C.E., Buermann W., Stenberg P., Voipio P., Smolander H., Häme T., Tian Y, Hu J., Knyazikhin Y., Myneni R.B. (2004): Evaluation of the MODIS LAI algorithm at a coniferous forest site in Finland. Remote Sensing of Environment, 91: 114–127.

Wang D., Wan B., Liu J., Su Y., Guo Q., Qiu P., Wu X. (2020): Estimating aboveground biomass of the mangrove forests on northeast Hainan Island in China using an upscaling method from field plots, UAV-LiDAR data and Sentinel-2 imagery. International Journal of Applied Earth Observation and Geoinformation, 85: 101986.

Wessels K.J., De Fries R.S., Dempewolf J., Anderson L.O., Hansen A.J., Powell S.L., Moran E.F. (2004): Mapping regional land cover with MODIS data for biological conservation: Examples from the Greater Yellowstone Ecosystem, USA and Pará State, Brazil. Remote Sensing of Environment, 92: 67–83.

Zhang Y., Gu F., Liu S., Liu Y., Li C. (2013): Variations of carbon stock with forest types in subalpine region of southwestern China. Forest Ecology and Management, 300: 88–95.

Zhang T., Su J., Liu C., Chen W.H., Liu H., Liu G. (2017): Band selection in Sentinel-2 satellite for agriculture applications. In: 23rd International Conference on Automation and Computing (ICAC). Huddersfield, Oct 26, 2017: 1–6.

Zhang Y., Ai J., Sun Q., Li Z., Hou L., Song L., Thang G., Li L., Shao G. (2021): Soil organic carbon and total nitrogen stocks as affected by vegetation types and altitude across the mountainous regions in the Yunnan Province, southwestern China. Catena, 196: 104872.

Zoran M., Stefan S. (2006): Atmospheric and spectral corrections for estimating surface albedo from satellite data. Journal of Optoelectronics and Advanced Materials, 8: 247–251.

Received: August 31, 2022
Accepted: May 11, 2023
Published online: July 10, 2023